ARCHIVES
of
FOUNDRY ENGINEERING

ISSN (2299-2944)
Volume 2023
Issue 4/2023

14 – 21

2/4

10.24425/afe.2023.146674

Published quarterly as the organ of the Foundry Commission of the Polish Academy of Sciences

Characterization of Ijero-Ekiti Quartz as Refractory Raw Material for Industrial Furnace

B.V. Omidiji [a, *], O.B. Ogundipe [b], H.A. Owolabi [a]
[a] Obafemi Awolowo University, Ile-Ife, Nigeria
[b] Landmark University, Omu-Aran, Nigeria
* Corresponding author: E-mail address: bvomidiji@gmail.com

Received 10.06.2023; accepted in revised form 27.07.2023; available online 07.11.2023

Abstract

This study investigated the suitability of Ijero-Ekiti quartz as a refractory raw material for industrial furnace applications. In order to ascertain its prospective applications, the thermal behaviour, mineralogical composition and chemical composition were determined. Ijero-Ekiti quartz was characterized using Fourier Transform Infrared Spectroscopy (FTIR), X-ray Diffraction (XRD), Thermogravimetric and Differential Thermal analysis (TGA and DTA). Its thermal conductivity with specific heat coefficient was determined. The outcome revealed that the quartz sample has a high purity of 94.3% SiO_2, making it suitable as a refractory material. The XRD analysis revealed the presence of alpha-quartz as the dominant crystal phase, which is desirable for refractory applications. The FTIR analysis indicated the absence of hydroxyl (-OH) groups. This indicates a low risk of failure and damage such as spalling, cracking and other forms of damage when produced into bricks. The TGA and DTA displayed significant mass losses and large endothermic bands, which were connected to the dehydroxylation of the quartz rock samples. Based on the demonstrated qualities, the quartz rock sample could be subjected to thermal processing. This study therefore established that Ijero-Ekiti quartz is a suitable raw material for refractory applications due to its high purity, alpha-quartz dominant crystal phase, absence of hydroxyl groups, and uniform morphology.

Keywords: Quartz, Refractory material, Industrial furnace, Thermal properties, Chemical composition

1. Introduction

Refractory raw materials (RRMs) industrial applications have rapidly grown over time, which is related to the growing demands for durable materials for high-temperature applications [1-3]. In the light of this development, numerous academics with a deep interest in the deployment of RRMs that are both high-performing and affordable have invested into developing a creative framework that would make RRMs available to users [1].

RRMs are generally understood to be substances that maintain their chemical identity, mechanical integrity, and dimensional stability when exposed to temperatures above 538 °C. They are also resistant to pressure loads, physical wear, chemical attack, and corrosion [4, 5]. The majority of RRMs are inorganic, non-metallic, polyphase materials with polycrystallinity, porosity, and heterogeneity as well. Typically, they are made of non-oxides or oxides of substances like magnesium (Mg), silicon (Si), zirconium (Zr), and aluminum (Al), among others. Alternately, one may say that they are made up of additives, a binder phase, and thermally stable mineral aggregates.

RRMs are widely used in the pyrometallurgical industry as construction materials (mostly linings) for furnaces, kilns, incinerators, and ovens. They are also used in service environments where thermomechanical stability is a top priority, such as flame

detector systems for rocket launch structures and re-entry heat shields for space shuttles [6, 5]. In the petrochemical sectors, they are also well suited for use as reactor and boiler liners [5, 6].
However, it has been stated that the iron and steel industry as well as the metal casting industry absorb roughly two-thirds of the RRMs generated globally. The most recent global refractories market report supports this [7]. According to the market analysis, the refractories market was valued in 2020 at $23.2 billion, and it is expected to increase by 2025 to $27.4 billion, with an annual compound growth rate of 3.4 percent by value [7].

In industries that use procedures that require elevated temperatures, choosing the right RRM is essential for maximizing productivity, energy efficiency, economic viability, manufacturing processes, and labor costs [8]. In the light of this knowledge, a variety of criteria must be considered while choosing the best RRM [9, 8]. A few of these variables in terms of physico-mechanical and chemical stability, installation-related challenges, production costs, and the required final product quality, among others affect the material performance. Finding RRM that can resist the challenging operational settings while remaining commercially viable is a challenge [9, 8]. Therefore, it's critical to have a solid grasp of the ideas behind the development, performance assessment, and failure features of RRMs.

Ijero-Ekiti Quartz is a mineral deposit located in Ijero-Ekiti, Ekiti State, Nigeria (Latitude: 7.8151 and Longitude: 5.0672). Minerals from this region have been reported to have high potential as refractory raw materials [10, 11]. Quartz as a silica mineral, has been widely used in the production of refractory materials due to its high melting point, thermal stability, and good chemical resistance [12]. Quartz has a high melting point of approximately 1700°C, which makes it ideal for use in high-temperature industrial furnaces [13]. Quartz is also chemically stable, making it resistant to chemical attack from many common industrial chemicals [14].
The characterization of Ijero-Ekiti Quartz as a refractory raw material for industrial furnaces is essential to evaluating its suitability for use in these applications. In this study, the chemical composition, mineral composition, and thermal properties of Ijero-Ekiti quartz were determined to evaluate its potential as a refractory raw material.

2. Materials and Methods

2.1. Materials

The material used for the study is quartz and was collected from the mining site in Ijero-Ekiti with the aid of a digger, shovel, and storage container.

2.2 Methods

The study involved several laboratory tests and experiments to determine the properties of Ijero-Ekiti quartz rock, its chemical composition and thermal stability. The examinations were conducted in accordance to American Standard for Testing Materials [15, 16] standards and guidelines.

The as-collected samples were sun-dried for 3 days to remove moisture content and as well facilitated easy grinding. The rock samples were mechanically milled in a laboratory ball mill into fine powders. To ensure complete evaporation of the unbounded moisture, the powders were heat-treated for 1 hour at 110℃ in an oven before the sample was taken to laboratory for further investigation and analysis.

The compositions of the quartz sample were investigated using FTIR, XRD, and X-ray fluorescence (XRF) spectroscopy. The quart sample's thermal stability was evaluated by exposing it to high temperatures and measuring its weight loss using TGA/DTA analysis. The study further investigated additional thermal characteristics including the sample's specific heat, heat transfer coefficient and thermal conductivity and diffusivity.

2.2.1. Fourier Transform Infrared Spectroscopy (FTIR)

The composition of the quartz sample was identified and characterized by measuring the infrared absorption or samples' emission by Fourier Transform Infrared Spectroscopy (FTIR) an effective and non-destructive test. The sample was subjected to FTIR infrared light, with a wavelength range of 10,000 to 100 cm^{-1}, part of which goes through while some were absorbed. The radiation absorbed by the molecules of the sample was converted into vibrational and rotational energy. The power source of the FTIR equipment was therefore turned on and its proper initialization was confirmed. The sample holder was cleaned by acetone with Kimwipes to ensure that there was no splash of the acetone on the instrument. The "spectrum" software was launched and "Spectrum 100" was selected on the software to begin the collection of data from signals. The resulting signal, which typically ranges from 650 to 4500 cm^{-1} and shows up as a spectrum at the detector, is the molecular fingerprint of the sample. The interactions between matter and electromagnetic radiation, which take the shape of a spectrum, are investigated using FTIR spectroscopy. Each molecule has a distinct spectral fingerprint that enables separation from other molecules [17]. The collected data was processed using the Fourier transform, a mathematical formula, to produce a spectrum that was examined to ascertain the sample's chemical composition.

2.2.2. X-ray diffraction (XRD)

The XRD analysis is based on passing X-ray beam through the rock sample. The d-spacing of the rock minerals, which is a function of the structural layers, is determined by the X-ray. The X-rays was directed at the prepared powdery samples, and they were diffracted in many directions. The pattern of the scattered X-rays was unique to the crystal structure of the rock sample, and was employed to recognize the sample's minerals.
First, the powdered samples were made into pellets and sieved to a size of 0.074 mm. Then, they were placed on a flat glass plate on an aluminum alloy grid (measuring 35 mm x 50 mm) and enclosed with paper. The samples were gently compressed by hand after wearing hand gloves. The Rigaku D/Max-lllC X-ray diffractometer, manufactured by Rigaku Int. Corp. in Tokyo, Japan, was used to analyze the sample. The diffractometer was set to produce diffractions at a scanning rate of 2^{o}/min at ambient temperature in the range of 2 to 50^{0}, with a CuKa radiation set at 20mA and 40kV. The obtained result of diffraction (relative intensity and d value) was compared to the ICDD mineral powder

diffraction file's standard data for minerals, which contains standard data for over 3000 minerals. In the diffractometer, the less than 2-micron sample fraction was grouped and the powder was pressed into an aluminum sample holder and rimed through a wide-angle Phillips P.W. 1011 goriometer connected to a PM 8220 recorder. Under the following instrumental conditions, scanning was performed from 2' to 40': Nickel filtered Fek and radiation, Recording/scanning rate of 1' 20 cm/min, voltage of 28 kv/12 mH, constant time and Range of 4 x 10 C.P.S

Finally, the reference table for conversion of 20 to d-values for the Fek alpha radiation in the JCPDC manual was used to interpret the diffractograms.

2.2.3. X- ray fluorescence (XRF)

The principle of quantum chemistry and atomic physics is used in this method. The sample was exposed to the full range of emitted photons from X-ray tube, resulting in the emission of fluorescence with the characteristic X-ray line spectra of the elements present in the specimens. To determine the intensities and energies of the lines emitted, a detection system was used. The rock sample was pulverized using a Herzog Gyro-mill (Simatic C7-621) for 60 seconds by first grinding 20g of the sample for 60 seconds with 0.4g of stearic acid. The Gyro-mill was then cleaned to avoid contamination after each grinding. Then, pellets were made by transferring the aluminum cup filled with the sample and 1g of stearic acid to the Herzong pelletizing equipment and pressed for 60 seconds at a pressure of 200 kN. The resulting 2 mm pellets were then placed in a sample holder of the x-ray equipment (Phillips PW-1800) for analysis.

2.2.4 TGA/DTA

Thermogravimetric analysis TGA is used to determine weight changes of a material as a function of temperature [18, 19]. The technique is employed to determine the composition and purity of the quartz material, as well as its thermal stability and decomposition mechanisms. Differential Thermal Analysis (DTA) is employed to determine difference in temperature between the sample and the reference material over time or with respect to temperature. The thermal properties of quartz material can be determined using this technique, such as its melting point, heat of fusion, and thermal expansion coefficient [20]. Both TGA and DTA can be employed to study the thermal behavior of the material, but the information provided by both are different. TGA provides information on the weight change of a material, while DTA provides information on the difference in temperature between a reference material and a sample [21, 22, 23, 24].

During this research work, 10mg prepared rock sample of was placed in an aluminum pan. The pan was then gradually heated at a rate of 10°C/min from ambient temperature up to 600°C while the weight loss was measured under a nitrogen atmosphere flowing at 50 cm3/min. The heating and cooling program consisted of a temperature range of 30°C to 220°C, followed by a reverse cooling from 220°C back to 30°C, both at a rate of 10°C per minute and held for 3 minutes. Equation 1 was considered in determining the degree of crystallinity (Xc) [25].

$$Xc = \frac{\Delta H_m}{(1-\Phi)\,\Delta H_m^0} \text{ x } 100\ \% \quad (1)$$

where ΔH_m^0 is the theoretical enthalpy of melting for 100%, Φ is the weight portion of the filler, and ΔH_m is the calculated enthalpy of melting for the sample.

2.2.5. Thermal Conductivity/Diffusivity, Heat Transfer Coefficient and Specific Heat Capacity:

The capacity of any material to conduct heat is measured by its thermal conductivity (TC). (Vaishnav, *et al*., 2022). Low thermal conductivity materials, such as insulators, are poor at conducting heat and are often used in thermal insulation [26, 27].

In this research, to measure the thermal conductivity of the Quartz sample a radial heat conduction apparatus (Armfield equipment model HT12) was employed with a service unit for heat transfer (Armfield equipment model HT10XC). This sample had a constant specific heat capacity of diameter 0.0018 and length 0.0043 m. The apparatus used a probe consisting of a thermocouple and a single heater wire. By applying a steady amount of electrical power to the heater, the wire's temperature increased in an exponential fashion. The rate of temperature increase over time was higher for samples with lower thermal conductivity and lower for those with higher thermal conductivity. Thus, the TC of the sample was calculated using the following equation based on the rate of temperature increase.

The thermal conductivity (λ) of the sample in [W/mK] was calculated by equation 2 [28].

$$\lambda = \frac{Q*X}{A\,(\Delta T)} \quad (2)$$

Where:
X: Thickness of sample [m]
Q: generated heat per unit length of sample/time [W]
A: Area [m^2]
ΔT: Temperature difference at time t0 and time t5 [K]

The heat transfer coefficient general definition is:

$$U = \frac{Q}{A*\Delta T} \quad (3)$$

Where:
Q: heat flux, W/m^2;
ΔT: temperature difference between the solid surface and surrounding fluid area, in K;
U: heat transfer coefficient, W/ (m^2•K)

The Heat Capacity Cp is also given by;

$$Cp = \frac{Q}{m*\Delta T} \quad (4)$$

Unit of Heat Capacity Cp is J/kg•ºC,
m: is the Mass (kg),
Q is change in energy (J), and
ΔT is Temperature change (ºC)

Thermal diffusivity, on the other hand, is a measure of how quickly heat can be transferred through a material. It is the ratio of

thermal conductivity to heat capacity. Diffusivity is the rate of diffusion measured as the rate at which heat is spread on a material.

Thermal Diffusivity α (m^2/s) is given as:

$$\alpha = \frac{\lambda}{\rho C_p} \quad (5)$$

Where:
Cp is the specific heat capacity (J/gK)
ρ is the density of the material and
λ : Thermal conductivity of sample [W/mK]

3. Results and Discussion

3.1. FTIR Analysis

The quartz rock sample was analyzed in the range of 400 to 4000 cm^{-1} using Fourier-transform infrared (FTIR) spectroscopy, and the results were presented in Figure 1. The spectrum indicated the presence of OH bonds in the form of water molecule, as evidenced by the weak hydroxyl peak at 2250 cm^{-1}. Also, the peak at 461 cm^{-1} and the strong absorption band between 1115-997 cm^{-1} corresponded to the bending vibrations and asymmetric stretching of Si-O-Si bonds, respectively. The spectral peaks at around 1635 cm^{-1} were identified as the O-H bending modes of the molecules of water adsorbed, as reported by [29]. At the surface of the quartz rock sample, the Si-OH stretching mode overlapped with the water bending vibration at approximately 1635 cm^{-1}, which result in the peak broadening at the frequency, as observed by [30] for unmodified quartz sand. These observations were consistent with the observations of [31] and suggested the presence of a silicate structure in the quartz rock sample.

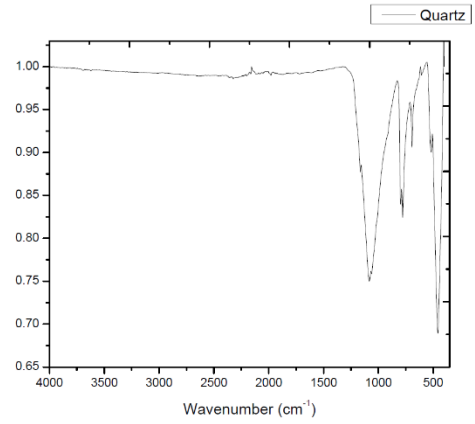

Fig. 1. FTIR spectra of Quartz

3.2 XRD Result Analysis

The outcome of X-ray diffraction (XRD) mineralogy of the quartz rock is as presented in Figure 2a. It was deduced from the result that quartz, albite, muscovite and illite are the primary constituents in the rock sample with quartz being the most abundant mineral in all the rock sample. These findings are pre-eminently supported by the several peaks of these minerals found in the respective diffractograms of the rock sample. Pie charts for the quartz rock sample is presented in Figure 2b for better visualization of the quantitative results. The results indicate that the quartz rock sample contains 92 % quartz, 1.3 % albite, 3.5 % muscovite and 4 % illite. From these results, it can be established that quartz rock sample with high quantities of orthoclase and albite belong to the tectosilicate mineral which forms igneous rocks. Correspondingly, these findings are supported by the observations in the XRF results. Another interesting spectacle is that these rock samples cannot only be used for high temperature insulation but can also be used for the manufacture of glass and ceramics [32].

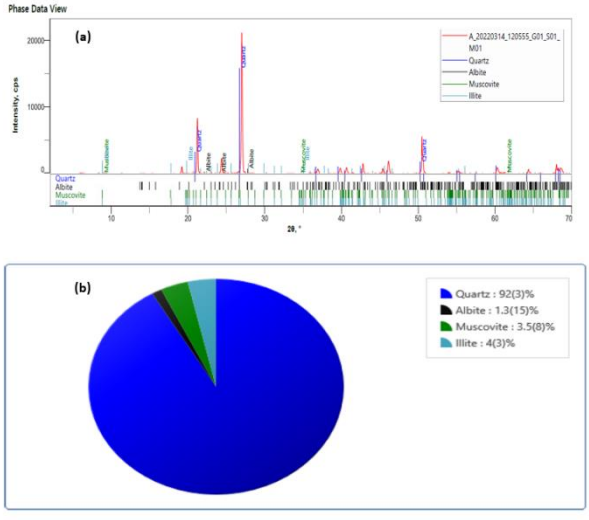

Fig. 2. XRD Phase Identification

3.3. XRF Result Analysis

Table 1 gives the chemical compositions of the quartz rock sample. The quartz has 94.30 SiO_2 wt. % and 2.4 wt. % Al_2O_3 alongside other oxides as its constituents. Thus, quartz's SiO_2 content is above the recommended content of SiO_2 for a Refractory material. However, this value is similar to what was observed in the work of [33] for Unwana beach silica sand which is an indication that this samples will be able to confer high melting point to the resultant refractory brick. Refractory materials that have high SiO_2 content greater than 46.51 wt. % possess the ability to withstand relatively high temperature which makes them suitable for elevated temperature applications with superior refractory properties [34]. Also, it is important to mention that the Al_2O_3 content in refractories has a direct linear relationship with the material's refractoriness such that the sample's refractoriness increases with increasing Al_2O_3 content. On the contrary, the presence of some coloured/fluxing oxides such as CaO, Na_2O_3, MgO, and K_2O, among others in high amount in a refractory material adversely affects refractoriness [35]. Correspondingly, how much of these oxides found in the sample under investigation follows the standard requirements for the production of refractory bricks for the lining of furnaces [36]. More importantly, previous studies have shown that clay samples with similar SiO_2 and Al_2O_3 contents belong to the alumino-silicate group of fireclays [37].

Table 1.
Chemical Composition of Quartz

Component Type	Conc (wt.%)	Mole (%)
SiO_2	94.303	95.990
Al_2O_3	2.379	1.427
V_2O_5	0.014	0.005
Cr_2O_3	0.087	0.035
MnO	0.023	0.020
Fe_2O_3	1.335	0.511
CuO	0.040	0.031
SO_3	0.553	0.422
CaO	0.307	0.335
K_2O	0.148	0.096
BaO	0.097	0.039
Ta_2O_5	0.045	0.006
Cl	0.617	1.065

3.4. TGA/DTA Analysis

The findings of the differential thermal analysis and thermogravimetric analysis (DTA and TGA) curve for quartz rock sample in the nitrogen atmosphere are shown in Figure 3. These curves indicate that quartz rock sample has good thermal properties. The DTA thermogram shows endothermic peak between 350°C and 450°C. This informed the last removal of the traces of OH^- in the form of H_2O which can exist above 600ºC [38, 39]. This also conforms to [40] that reported the dehydroxylation of the minerals in the Aloji Fireclay at 639.67°C. The TGA results reveal a single loss of mass in the region of 400 to 450°C for the quartz sample amounting to a loss of 22.0% which is a favourable result. The loss corresponds to the removal of the sample's water molecules, which is in tandem with the findings of [41]. There is no specific TGA value that is good or suitable for all refractory materials, as the suitability of a particular material will depend on its intended use [38]. For example, a refractory material with a higher decomposition temperature and a slower rate of decomposition may be more suitable for use in high-temperature environments, while a material with a lower decomposition temperature and a faster rate of decomposition may be more suitable for use in lower-temperature environments. Therefore, the TGA analysis for the quartz shows that the sample has good thermal stability.

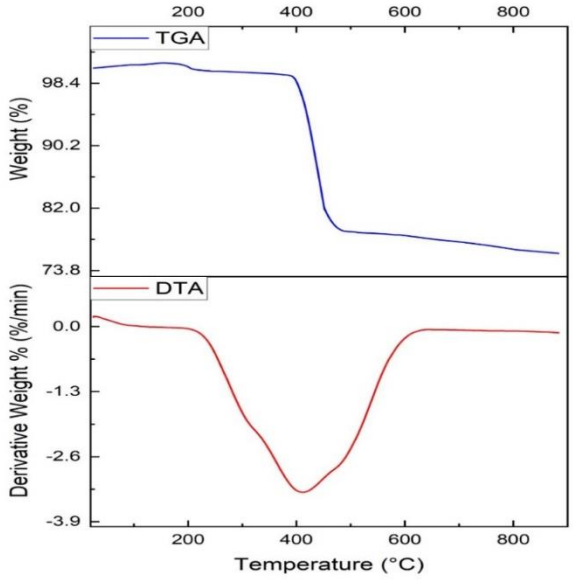

Fig. 3. Curve change for TGA/DTA of quartz sample in the nitrogen atmosphere

3.5.Thermal Conductivity/Diffusivity, Heat Transfer Coefficient and Specific Heat Capacity

The thermal diffusivity and conductivity of Ijero-Ekiti quartz were found to be 55 mm^2/s and 0.25 W/mK, respectively as presented in Table 2. These values indicate that Ijero-Ekiti quartz has good thermal conductivity and diffusivity, which are desirable properties for a refractory material [42]. Also, the heat transfer coefficient of Ijero-Ekiti quartz was found to be 25.5 W/m^2K. This value indicates that Ijero-Ekiti quartz has a high coefficient of heat transfer, which is desirable for efficient transfer heat in industrial furnaces. The specific heat of the sample was found to be 6.67 J/kgK. This value indicates that Ijero-Ekiti quartz has a relatively low specific heat, which means that it can heat up quickly and does not require a large amount of heat to raise its temperature [43]. The thermal conductivity, diffusivity, heat transfer coefficient and specific heat of Ijero-Ekiti quartz was found to be similar to other

refractory materials such as alumina and silica. The thermal response of the material to when heat energy is added to or removed from a material can result in changes in temperature, dimensions, and heat conduction. For refractory materials, the ability to conduct heat, the coefficient of thermal diffusivity and the specific heat capacity are essential properties that determine their performance [42, 44].

The study revealed a reduction in thermal diffusivity within acceptable limits, which is favorable as materials with high thermal diffusivity tend to adapt quickly to ambient temperature due to faster heat transfer. Materials that have low thermal diffusivity respond slowly, taking longer to reach a new equilibrium state whereas those has higher thermal diffusivity respond rapidly to thermal changes in their environment [45, 46, 47].

Based on the experimental measurements of thermal conductivity, diffusivity, heat transfer coefficient, and specific heat, Ijero-Ekiti quartz exhibits desirable thermal properties for use as a refractory material for industrial furnaces. Its high thermal conductivity and diffusivity, high heat transfer coefficient, and relatively low specific heat make it a suitable candidate for applications that require high-temperature resistance and efficient heat transfer [48, 49, 50].

Table 2.
Specific Heat, Heat Transfer Coefficient, Thermal Diffusivity and Conductivity

Thermal Properties	**Value**
Specific Heat (Cp)	0.006667275 J/gK
Heat Transfer Coefficient (U)	25.53675572 W/m^{2}K
Thermal conductivity (λ)	0.255367557 W/mK
Thermal Diffusivity (α)	55.567155 mm^2/s

4. Conclusions

The characterization of Ijero-Ekiti Quartz as a refractory raw material for industrial furnaces revealed that the sample has several desirable properties for use in high-temperature industrial furnaces. The XRF analysis showed that the sample was composed primarily of silicon dioxide, with minor amounts of aluminum oxide, iron oxide, and titanium dioxide, which have been reported to enhance its thermal stability and resistance to chemical attack. The XRD analysis showed that the sample was primarily composed of quartz and albite with a trace of muscovite, and illite, which have also been reported to enhance its thermal stability and resistance to chemical attack. The TGA/DTA analysis showed that the sample had a low thermal expansion, which makes it resistant to thermal shock and less prone to cracking when subjected to rapid temperature changes, and low thermal conductivity, which makes it an effective insulating material.

Overall, the characterization of Ijero-Ekiti Quartz as a refractory raw material for industrial furnaces provides strong evidence that it has the potential to be used as a high-temperature refractory material in industrial furnaces.

References

[1] Jongs, L.S., Jock, A.A., Ekanem, O.E. & Jauro, A. (2018). Investigating the industrial potentials of some selected Nigerian clay deposits. *Journal of Minerals and Materials Characterization and Engineering*. 6, 569-586. DOI: 10.4236/jmmce.2018.66041.

[2] Adeoti, M., Dahunsi, O., Awopetu, O.O., Aramide, F., Alabi, O., Johnson, O. & Abdulkarim, A. (2019). Suitability of selected Nigerian clays for foundry crucibles production. *Procedia Manufacturing.* 35, 1316-1323. https://doi.org/10.1016/j.promfg.2019.05.023.

[3] Thethwayo, B. & Steenkamp, J. (2020). A review of carbon-based refractory materials and their applications. *Journal of the Southern African Institute of Mining and Metallurgy*. 120, 641-650. http://dx.doi.org/10.17159/2411-9717/1011/2020.

[4] Fleuriault, C., Grogan, J. & White, J. (2018). Refractory materials for metallurgical Uses. *The Journal of The Minerals, Metals & Materials Society*. 70, 2420-2421. https://doi.org/10.1007/s11837-018-3096-5.

[5] Sarkar, R. (2016). *Refractory technology: Fundamentals and applications*. CRC Press, Boca Raton, Florida, United State.

[6] Lee, S. (2015). Types of Refractory Materials and their Applications [Online]. Linkedin. Available: https://www.linkedin.com/pulse/types-refractory-materials-applications-le-sylvia [Accessed June 16 2021]

[7] MARKETS AND MARKETS. (2020). Refractories Market by Form (Shaped Refractories, Unshaped Refractories), Alkalinity (Acidic & Neutral. Basic), End-Use Industry (Iron & Steel, Power Generation, Non-Ferrous Metals, Cement, Glass), and Region - Global Forecast to 2025 [Online]. MARKETSANDMARKETS. Available: https://www.marketsandmarkets.com/Market-Reports/refractories-market-222632393.html?gclid=CjwKCAjwiLGGBhAqEiwAgq3q_mu5-rTCddXNmL2Po9LaVwDTS2rVmPj8dfITLtQzmA4u7BCHkVKZ-RoCur0QAvD_BwE [Accessed June 16 2021].

[8] Ren, C. & Enneti, R.K. (2020). Process design and material development for high-temperature applications. *The Journal of The Minerals, Metals & Materials Society*. 72. 4028-4029. https://doi.org/10.1007/s11837-020-04381-4.

[9] Patel, N. (2013). Factors affecting the lifespan of cast refractory linings: a general overview. *Journal of the Southern African Institute of Mining and Metallurgy*. 113, 637-641.

[10] Oyeyemi, A.O., Adekola, F.A., & Olaleye, M.B. (2016). Characterization of Ijero-Ekiti kaolin for industrial applications. *Journal of Minerals and Materials Characterization and Engineering*. 5(3), 153-160. https://doi.org/10.4236/jmmce.2016.53018.

[11] Adeniyi, F.I., Ogundiran, M.B., Hemalatha, T. & Hanumantrai, B.B. (2020). Characterization of raw and

thermally treated Nigerian kaolinite-containing clays using instrumental techniques. *SN Applied Sciences*. 2, 1-14. https://doi.org/10.1007/s42452-020-2610-x.
[12] Kralik, G., Martins, K.V., Alves, J.R., Sartori, D.V., Scholz, R. & Corat, E.J. (2016). Characterization and utilization of quartz sands in the manufacture of silicon metal. *Journal of Cleaner Production*. 112, 3304-3311. https://doi.org/10.1016/j.jclepro.2015.06.108.
[13] Guan, Y., Zhang, X., Chen, J. & Wang, L. (2018). Study on thermal shock resistance and high-temperature behavior of quartz-feldspar refractory materials. *Journal of the American Ceramic Society*. 101(4), 1467-1475. https://doi.org/10.1111/jace.14900.
[14] Zhou, C., Gao, X., Xu, Y., Buntkowsky, G., Ikuhara, Y., Riedel, R., & Ionescu, E. (2015). Synthesis and high-temperature evolution of single-phase amorphous Si–Hf–N ceramics. *Journal of the European Ceramic Society*. 35(7), 2007-2015. https://doi.org/10.1016/j.jeurceramsoc.2015.01.026.
[15] ASTM C201-93(2019). *Standard test method for thermal conductivity of refractories.* ASTM International, West Conshohocken, PA, United State.
[16] ASTM C114-22 (2022). *Standard test methods for chemical analysis of hydraulic cement.* ASTM International, West Conshohocken, PA, United State.
[17] Griffiths, P.R. & De Haseth, J.A. (1986). *Fourier transform infrared spectrometry*. John Wiley & Sons; New York, United State.
[18] Stodghill, S.P. (2010). Thermal analysis - A review of techniques and applications in the pharmaceutical sciences. *American Pharmaceutical Review*. 13(2), 29-36.
[19] Craig, D.Q.M., Reading, M. (2007). *Thermal analysis of pharmaceuticals*. CRC Press, Taylor and Francis Group, Boca Raton, Florida, United State.
[20] Drábik, M. (2017). The challenge of methods of thermal analysis in solid state and materials chemistry. *Pure and Applied Chemistry*. 89(4), 451-459.
[21] Drabik, M. & Slade, R.C. (2004). Macrodefect-free materials: modification of interfaces in cement composites by polymer grafting. *Interface Science*. 12(4), 375-379. https://doi.org/10.1023/B:INTS.0000042335.65518.11.
[22] Mojumdar, S.C., Mazanec, K. & Drabik, M. (2006). Macro-defect-free (MDF) cements. *Journal of Thermal Analysis and Calorimetry*. 83(1), 135-139.
[23] Drábik, M. (2009). Contribution of materials chemistry to the knowledge of macro-defect-free (MDF) materials. *Pure and Applied Chemistry*. 81(8), 1413-1421. https://doi.org/10.1351/PAC-CON-08-07-16.
[24] Drabik, M., Billik, P. & Galikova, L. (2012). Macro defect free materials; the challenge of mechanochemical activation. *Ceramics-Silikáty*. 56(4), 396-401. https://doi.org/10.1007/s10973-005-7045-5.
[25] Ahmed, Y.E., Abdulaziz, A.A., Hamid, M.S., Anesh, M.P., Saeed, M.A., Arfat, A. & Mohammad, I.A. (2019). Effect of pyrolysis temperature on biochar microstructural evolution, physicochemical characteristics, and its influence on biochar/polypropylene composites. *Applied Science*. 9(6), 1-18. https://doi.org/10.3390/app9061149.
[26] Ajala, A.J. & Badarulzaman, N.A. (2016). Thermal conductivity of Aloji fireclay as refractory material. *International Journal of Integrated Engineering*. 8(2), 16-20.
[27] Vaishnav, H., Navin, K., Kurchania, R. & Ball, R.J. (2022). Synthesis of ZrO_2 based nanofluids for cooling and insulation of transformers. *IEEE Transactions on Dielectrics and Electrical Insulation*. 29(1), 199-205. DOI: 10.1109/TDEI.2022.3148444.
[28] Ajiboye, T.K., Fabiyi, M.O., Mustapha, N. & Abdulkareem, S. (2022). Characterization of clay and granite dust blends as novel materials for energy storage and diffuser in constructing solar flat-plate collector. *Tanzania Journal of Science*. 48(2), 283-293.
[29] Ritz, M., Vaculíková, L. & Plevová, E. (2010). Identification of clay minerals by infrared spectroscopy and discriminant analysis. *Society for Applied spectroscopy*. 64(12) 1379-1387.
[30] Yue, C., Liu, J., Zhang, H., Dai, L., Wei, B. & Chang, C. (2018). Increasing the hydrophobicity of filter medium particles for oily water treatment using coupling agents. *Heliyon*. 4(9), 1-14. DOI: 10.1016/j.heliyon.2018.e00809.
[31] Zaitan, H., Bianchi, D., Achak, O. & Chafik, T. (2008). A comparative study of the adsorption and desorption of o-xylene onto bentonite clay and alumina. *Journal of Hazardous Materials*. 153(1-2), 852-859. https://doi.org/10.1016/j.jhazmat.2007.09.070.
[32] Gao, J., Jiang, C. & Zhang, X. (2007). Kinetics of curing and thermal degradation of POSS epoxy resin/DDS system. *International Journal of Polymeric Materials and Polymeric Biomaterials*. 56(1), 65-77. https://doi.org/10.1080/00914030600710620.
[33] Odewole, P.O., Kashim, I.B. & Akinbogun, T.L. (2019). Production of refractory porcelain crucibles from local ceramic raw materials using slip casting. *International Journal of Engineering and Manufacturing*. 9(5), 56-69. DOI: 10.5815/ijem.2019.05.05.
[34] Oluwagbenga, O.P. & Majiyebo, A.E. (2019). Development of aluminosilicate refractory crucibles from the optimum mix of Awo quartz and Ikere Ekiti clays. *ATBU Journal of Science, Technology and Education*. 7(2), 331-340.
[35] Shuaib-Babata, Y.L., Ibrahim, H.K., Ajao, K.S., Elakhame, Z.U., Aremu, N.I. & Odeniyi, O.M. (2019). Assessment of physico-mechanical properties of clay deposits in Asa Local Government Area of Kwara State Nigeria for industrial applications. *Journal of Research Information in Civil Engineering*. 16(2), 2727-2753.
[36] Aremu, D.A., Aremu, J.O. & Ibrahim, U.H. (2013). Analysis of Mubi clay deposit as furnace lining. *International Journal of Scientific and Technology*. 2(12), 183-186.
[37] Olajide, O.I., Michael, O.B. & Terna, T.D. (2015). Production and characterization of aluminosilicate refractory brick using Unwana beach silica sand, Ekebedi and Unwana clays. *British Journal of Applied Science & Technology*. 5(5), 461-471.
[38] Osabor, V.N., Okafor, P.C., Ibe, K.A. & Ayi, A.A. (2009). Characterization of clays in Odukpani, south eastern Nigeria. *African Journal of Pure and Applied Chemistry*. 3(5), 79-85. ISSN 1996 – 0840.
[39] Tenimu, A.A. (2019). Thermogravimetric and differential thermal investigation of rice husk cellulose. *Bayero Journal*

of Pure and Applied Sciences. 12(1), 6-11. http://dx.doi.org/10.4314/bajopas.v12i1.2.
[40] Amkpa, J.A. & Badarulzaman, N.A. (2016). Thermal conductivity of Aloji fireclay Brick. *International Journal of Integrated Engineering*. 8(3), 16-20.
[41] Silva, K.R, Liszandra, F.A., Camposb, L.N. & Santanaa, D.L. (2019). Use of experimental design to evaluate the effect of the incorporation of quartzite. residues in ceramic mass for porcelain tile production. *Materials Research*. 22(1), 1-11. https://doi.org/10.1590/1980-5373-MR-2018-0388.
[42] Czichos, H., Saito, T., Smith, L.E. (2011). *Springer handbook of metrology and testing*. Springer, New York, United State.
[43] Navas, V. G., Sandá, A., Sanz, C., Fernández, D., Vleugels, J., Vanmeensel, K., & Fernández, A. (2015). Surface integrity of rotary ultrasonic machined ZrO_2–TiN and Al_2O_3–TiC–SiC ceramics. *Journal of the European Ceramic Society*, 35(14), 3927-3941. https://doi.org/10.1016/j.jeurceramsoc.2015.06.018.
[44] Palm, M. & Inden, G. (1995). Experimental determination of phase equilibria in the Fe Al C system. *Intermetallics*. 3(6), 443-454. https://doi.org/10.1016/0966-9795(95)00003-H.
[45] Wulf, R., Barth, G. & Gross, U. (2007). Intercomparison of insulation thermal conductivities measured by various methods. *International Journal of Thermophysics*, 28, 1679-1692. https://doi.org/10.1007/s10765-007-0278-8.
[46] Incropera, F.P., DeWitt, D.P., Bergman, T.L., Lavine, A.S. (2007). *Fundamentals of heat and mass transfer*. John Wiley & Sons; New York, United State.
[47] Hagemann, L. & Peters, E. (1982). Thermal Conductivity-comparison of methods: ASTM-method, hot wire method and its variations. *Interceram*. 31, 131-135.
[48] Ferber, M.K., Weresczak, A.A. & Hemrick, J.G. (2006). *Comprehensive creep and thermophysical performance of refractory materials*. United States. DOI:10.2172/885151.
[49] Litovsky, E., Kleiman, J.I. & Menn, N. (2003). Measurement and analysis by different methods of apparent, radiative, and conductive thermophysical properties of insulation materials. *High Temperatures-High Pressures*. 35(1), 101-108. DOI:10.1068/htjr080.
[50] Arthur, E.K. & Gikunoo, E. (2020). Property analysis of thermal insulating materials made from Ghanaian anthill clay deposits. *Cogent Engineering*. 7(1), 1-20. https://doi.org/10.1080/23311916.2020.1827493.